PHASE DETERMINATION OF HARMONIC COMPONENTS OF CURRENT ASSOCIATED TO MECHANICAL UNBALANCED ROTORS WHILE COUPLED TO AN INDUCTION MOTOR

Alfonso C. García Reynoso[1,2], Enrique Ladrón de Guevara Durán[1,2], Alfonso García Portilla[1], Alberto P. Lorandi Medina[2], Guillermo Hermida Saba[2]

[1]Instituto Tecnológico de Veracruz, Miguel Ángel de Quevedo 2779, C.P. 91860, Veracruz, Ver. México
Tel. y Fax (229) 9385764,
[2]Instituto de Ingeniería de la Universidad Veracruzana, Juan Pablo II s/n Boca del Río, Veracruz, 94294 México, e-mail: garreynoso@hotmail.com

Correspondence concerning this article should be addressed to
Alfonso C. García Reynoso, Avenida Costa Verde 832, CP 94294 Boca del Río, Veracruz, México.
E-mail: algarcia@uv.mx

Abstract

An improvement to the method for single-plane rotor balancing which requires some components of the electric signal spectrum from each phase of the electric motor to which it is directly coupled is developed. The signal readings, which are scalar quantities that reflect residual complex values (offset with magnitude and phase) when there is no imbalance, produce a nonlinear behavior of the data with respect to the unbalance forces. This requires an algorithm to determine, based on readings of residual values for the balanced condition, and the imbalanced rotor, the complex values that directly relate to the imbalance. From here the influence coefficients and balancing masses are calculated. This algorithm was verified by running two study cases, with satisfactory results.

Keywords: Single Plane Balancing, Induction Motors, Current Harmonics.

Nomenclature

F_0 Force produced by Original unbalance at work radius

F_2 Force produced by original unbalance plus the trial weight 2

W_{p_2} Trial mass 2

N Measured current, milliamps, original unbalance

N_2 Measured current, milliamps with trial weight 2

θ_i Phase angle

Introduction

The relationship among the spectral harmonics of an electric current induction motor, and its mechanical and electromagnetic problems is well known. In 1995, Dorrel [1] studied how the magnitude of electric harmonics related to the mechanical harmonics in motors focusing on eccentricity.

In 1997, Riley [2], [3] and [4], analyzed these relations to establish limits for the electric harmonics as they correlate with vibrations, concluding there is a monotone relationship between these two variables. Caryn in 1997 finds, based on theoretical as well as on experimental bases, that there is a linear relationship between specific electric harmonics with mechanical vibration. Additionally, in 1999 he presents an analysis including the effect of externally induced vibrations. Finley [5] in 2000 makes a complete analysis of the relation among electric harmonics and mechanical problems including misalignment, unbalance, bearings failure, fractured rotor bars, etc. In 2004 Kral [6] proposes a technique to estimate unbalance using harmonics that are present in the electric power, showing positive results in assessing static and dynamic unbalance. In 2007 Neelam [7] presents an analysis of the electric current as the most popular for failure diagnosis not only electrical but mechanic as well showing effectiveness to determine abnormal operation of induction motors, including situations involving gear trains. In 2008 Bellini [8] presents a paper review of the previous ten years showing a list of references and research activity classified in four topics: a) electric failures, b) mechanical failures, c) signal processing for monitoring and analysis, and d) technical decision using artificial intelligence. In 2009 Camargo [9] presents results of single-plane rotor using electric harmonics that relate to mechanical unbalance.

García [10] in 2010 develops an algorithm that uses magnitudes of harmonic components of electric current to determine the influence coefficients and the balance masses of a directly coupled rotor. The procedure requires three trial weights to carry on balancing.

Instrumentation

The measurement system has the following elements: Hall-effect probes for electric current, signal conditioning, data acquisition card, and virtual instrument developer in G-language.These elements are described below.

Signal conditioning is performed by a set of transformers connected in star, and a set of operational amplifiers for gain control. The basic scheme for each channel is shown in figure 1.

The dataacquisition card is described in table 2.

The virtual instrument is developed in Labview 8.6, and it has user-friendly displays allowing reading and saving of desired information.

It consists of the following parts:

1. Data type specification according to the acquisition card, and to the system to be measured.
2. Instrument calibration.
3. Input signal display.
4. Filter configuration.
5. Filtered signal display.
6. Spectrum plots before and after filtering.
7. Harmonic vectors display.
8. File specification of records.

Next figures 2 to4 show some of the above mentioned displays:

The experimental work conducted to validate this proposed method was based on two electric motors whose characteristics are shown in tables 3 and 4.

Measurement of residual current signals

A residual current is considered as the remaining harmonics after subtracting the fundamental current circulating in a motor wiring. These harmonics are due to different effects, mechanical and electrical, as has been reported for some time [5][8].

These currents are produced by a deformation of the magnetic field in the motor air-gap, as a result of mechanical unbalance. However, the residual condition is also obtained by motor eccentricity, asymmetry of coil structure of stator and rotor, that is, due to static and dynamic irregularities in the air-gap [2][8].

By means of the sensing system, the fundamental current consumed by the motor, and the harmonics produced by the mechanical and the electromagnetic problems are obtained. The Fourier spectrum of the signal is displayed and the mechanical unbalance is indirectly determined by filtering the associate harmonics.

The measurement system is formed by a virtual instrument, a set of sensors and its signal conditioning. It is designed for 220 volts and a maximum of 15 amperes. Voltage is monitored by a set of transformers connected in star with magnetic cores that respond to a maximum of 10 kHz. The electric signal is obtained through Hall-effect probes which have a range of 10 kHz.

Depending on harmonic order, there is an associated mechanical or electromagnetic problem. Of particular interest is the harmonic related to mechanical unbalance. These harmonics depend on the rotor slip, input frequency, and they occur at the frequencies h_1 and h_2 given by the following expressions:

$$h_1 = f_s + f_r \quad (1)$$

$$h_2 = f_s - f_r \quad (2)$$

where:

f_r = Rotor angular velocity in revolutions per second

f_s = Line frequency of motor

h = Harmonic frequency that relates to mechanical unbalance

Once the harmonic frequencies are obtained, signal is filtered with an IIR filter with a similar configuration as the Butterworth analog filter to obtain a more precise behavior of these harmonics.

This instrument was validated with commercial ampere-meters, and calibration was performed through an electronic circuit that conditions the signal using software.

During the tests, measurements were taken in five-minute samples for each run. Because the signal has large variations, that requires using the root mean square (RMS) to get a representative value.

Characteristics of the spectral values of electric current

Due to the fact that harmonic magnitudes do not converge to zero for a balanced rotor, as mechanical vibrations do, they show an offset which may be different for the three current lines, when unbalance is present, the measured values of harmonics do not follow a linear relationship with the unbalance forces. However, after the offset is removed, the relation is approximately linear as shown in figure 5 for a test case. In this figure, the lower curve has the offset removed (as will be described below), and it tends towards the origin as the unbalance tends to zero. This corrected curve is nearly linear and homogeneous, as mechanical unbalance is.

The subtraction process of offset requires knowing the phase (complex values) of the harmonics, which in these measurements are not determined directly, but in a relative mode. This subtraction process is numerical as described below.

Measurement of Relative Phase angle

The filter that gets the harmonics related to unbalance has an analog structure Butterworth. This filter maximizes amplitude in the band pass, and the response decays linearly from the cut-off frequency towards minus infinity. For a first order filter, it is -20dB per decade (-6dB per octave) and it keeps its shape for higher orders (with a steeper fall-off from the cut-off frequency). This is the most important reason why this filter structure was selected, since it lets to observe with clarity the relationship between harmonics and unbalance masses.

The phase response does not have these advantages due to phase lag for each filter order, which is 45° at cut-off. It was considered that the filter-lag effect is the same for each of the line frequencies; therefore the relative phase angles among harmonics can be measured.

Since harmonics have the same frequency, Hilbert transform was used to determine its relative angles, considering phase A as a reference with an arbitrary value of 0°.

It may be observed, for harmonics of a balanced-rotor condition that the relative phase angles among them (L_1, $L_2$and L_3) have values of 120° (low frequency). However, when unbalance is present these relative phase angles change due to the vector sum of the offset and the unbalance effect. Figure 6 shows signal time-histories for a given unbalance.

Assuming that the three vectors (L_1, L_2 and L_3) must arrange with 120° among them, when offset is subtracted (R_{0L1}, R_{0L2} andR_{0L3}), with absolute phase angles that depend on unbalance, and taking as a reference the balanced-rotor condition with angular positions 0°, 120° and 240° respectively (B_1, $B_2$and B_3), vectors may look like is shown in figure 7.

When direct measurements are included, vectors may look like shown in figure 8 and equations are:

$$P_{0L1} = B_1 + R_{0L1} \quad (3)$$

$$P_{0L2} = B_2 + R_{0L2} \quad (4)$$

$$P_{0L3} = B_3 + R_{0L3} \quad (5)$$

To obtain the absolute phase angles, the algorithm uses the relative phase angles among vectors P_{0L1}, P_{0L2} andP_{0L3}obtained by measurement. It then iterates until vectors R_{0L1}, R_{0L2}andR_{0L3} reach 120° among them, satisfying the following conditions:

$$\frac{R_{0L2}}{R_{0L1}} = \frac{B_2}{B_1} \qquad \frac{R_{0L3}}{R_{0L1}} = \frac{B_3}{B_1} \quad (6)$$

There is a unique vector combination that fulfills this condition, and thus the absolute phase angles are determined.

Single plane balancing

Having determined the harmonic phases, it is possible to calculate the influence coefficients as well as the balance masses for each combination of trial weights. In the traditional method of influence coefficients formulas (7) and (8) provide a balance mass assuming the magnitude and phase are known.

$$A_2 = \frac{N_2 - N}{W_{p_2}} \quad (7)$$

$$W_{c_2} = -\frac{N}{A_2} \quad (8)$$

Each line has its influence coefficient which gives a balance mass. The average is:

$$W_{prom} = \left(W_{c_2} + W_{c_4} + W_{c_6}\right)/3 \quad (9)$$

The algorithm has the following sequence:

1. It determines absolute phase angle for each harmonic applying equations (3) to (6).
2. It calculates influence coefficients and balance masses using formulas (7) to (9).
3. The average balance mass gives a better estimation as shown in the test cases.

Applications

The first series of tests was conducted with a rotor coupled to an induction motor whose characteristics are described in table 3.

Initially the rotor was balanced and its corresponding harmonics were measured.Then an unbalance mass of 8.5 grams was positioned in several angular positions, at the same radius, as shown in table 2 where 24 test runs were recorded, with increments of 15°.Each measurement took 39,999 data for every phase and for high and low frequencies. RMS values of amplitudes are shown in table 5.

Relative phase angles were also measured as is shown in table 6.

These data are fed into the algorithm to get the influence coefficients displayed graphically in figure9. The average values are shown in table7.

With this average influence coefficient the algorithm calculates balance masses for every angular position of applied unbalances to obtain results of table 8 as well as of figure 10.

A second series of tests deals with a rotor coupled to another induction motor whose data are shown in table 4. An unbalance mass of 8.5g $\angle 0°$ is applied, and a trial mass of 4.3 g is placed in several angular positions to make a total of eight test runs. Measurements are shown in tables 9 and 10.

The resulting balance masses are shown in table 11.

Conclusions

1. Based on previous work of other researchers, where a relationship between the mechanical unbalance and the electric-current harmonics is reported, it is developed in this article a more efficient method of balancing that uses the rms values of these harmonics and the relative phase angles among the three frequency lines.
2. This balancing technique faces two problems, one is data variations of samples which is solved by taking three to five minute sampling, and calculating the rms value of the response. The other difficulty is nonlinearity of data due to an offset.
3. The magnitudes of the signal spectrum do not have a linear homogeneous relationship with the unbalance force due to a complex offset that can be measured with the balanced rotor, and that adds to the unbalance effects. These vectors are measured in magnitude, and their measured phase angles are relative.
4. The harmonics of the balanced-rotor condition are determined in magnitude, and their phase angles are set to 0°, -120° and -240° for the corresponding line frequency L_i, in the case of low frequency (h_2). For high frequency (h_1) the relative angles are set to 0°.
5. The harmonics related to the unbalance condition (vectors P_{0L1}, P_{0L2} and P_{0L3}) have an absolute phase that is iteratively calculated depending on the parameter α_1, which is the absolute phase angle of line L_1 and taking into account the relative phase with the other frequency lines.
6. The numerical sequence consists of varying phase angle α_1 of L_1 until the relative phase angles among the three corrected vectors R_{0L1}, R_{0L2} andR_{0L3} satisfy conditions (6). Thus the absolute phase angles are determined.
7. This balance system saves the influence coefficients in order to apply them in subsequent balances when monitoring current spectra and determining at any time the actual balance masses.

8. Test cases conducted with a directly coupled rotor to an induction motor show results whose average converge to the expected balance masses.
9. The virtual instrumentdeveloped in this project is of low cost and it may have some potential for industrial applications.

References

[1] Dorrell D. G.,ThomsonW.T.,Roach S. (1995). Analysis ofAirgap Flux, Current And Vibration Signals As A Function Of The Combination of Static And Dynamic Airgap Eccentricity In 3 Phase Induction Motors. IAS 95 Conference record of the 1995 IEEE Industry Applications Conference Vol. 1 pp 563-570.

[2] Riley C. M, Lin B. K,Habetler T.G and Kliman G.B. (1997). Stator Current Based Sensorless Vibration Monitoring Of Induction Motors.Applied Power Electronics conference and exposition, Vol. 1 pp 142-147.

[3] Riley C.M, Lin B. K., Habetler T. G. (1998). A Method ForSensorless On-Line Vibration Monitoring Of Induction Machines.IEEE Transactions on Industry Applications, Vol. 34, No. 6.

[4] Riley C.M, Lin B. K., Habetler T. G. (1999). Stator Current Harmonics And Their Causal Vibrations: A Preliminary Investigation Of Sensorless Vibration Monitoring Applications. IEEE Transaction on Industry Applications,Vol.35 No. 1.

[5] Finley W., Hodowanec M.,Holter W. (2000). An Analytical Approach To Solving Motor Vibration Problems. IEEE Transaction On Industry Applications, Vol. 36 No. 5.

[6] Kral C., Habetler T. G., Harley R. (2004). Detection Of Mechanical Imbalance Of Induction Machines Without Spectral Analysis Of Time Domain Signals. IEEE Transaction on Industry Applications, Vol. 40 No 4.

[7] Neelam M., Dahiya R. (2007). Motor Current Signature Analysis And Its Applications In Induction Motor Fault Diagnosis. International Journal of Systems Applications Engineering & Development, Vol. 2.No. 1.

[8] Bellini A., Filippeti F., Tassoni C., Capolino G. A.(2008). Advances in Diagnostic Techniques for Induction Machines, IEEE Transactions on Industrial Electronics Vol. 55.No. 12.

[9] Camargo M. J., García R.A.,Ladrón de Guevara D. E., Hernández M.E. (2009). Balanceo Dinámico De Motores De Inducción Utilizando Componentes De Corriente Eléctrica, XV Congreso Internacional Anual de la SOMIM, Instituto Tecnológico Superior de Cajeme, Cd.Obregón, Sonora, No. A4_21.

[10] García R. A., Ladrón de Guevara D. E., Ceballos G. R., Camargo M. J., Hernández M. E., García P. A. (2010). Método De Balanceo Dinámico, En Un Plano, De Rotores Acoplados Directamente A Un Motor De Inducción Empleando Datos De Corriente Residual. XVI Congreso internacional anual de la SOMIM,Universidad Autónoma de Nuevo León, Monterrey, Nuevo León, México,No.A4-94

Table 1 Characteristics of current probe FWBELL M-15 [6]

Range of measurement	15 A
Sensitivity	0.09 V/A to 0.14 V/A
Overload capacity	25 A
Input Voltage	+5.0 V +/- 0.5 V
Offset	2.5 V +/- 0.3 V
Frequency Range	CD to 20 kHz

Table 2 Data acquisition card NI-USB 233

Resolution	24-bit
Dynamic Range	102 dB
Sampling rate per channel	50 kS/s max
Analog inputs	4 simultaneous
Input range	±5 V

Table 3 Induction Motor No.1

Power	0.5 H.P.
Voltage	220 V 3ϕ
Current	1.8 A
Nominal Velocity	1750
Frequency	60 Hz
Manufacturer	Siemens
Connection	YY

Table 4 Induction Motor No.2

Power	0.75 h.p
Voltage	220 V 3ϕ
Current	3.0 A
Nominal Velocity	1730
Frequency	60 Hz
Manufacturer	Siemens
Connection	YY

Table 5 Harmonic values of test runs, mA, highfrequency h_1.

Case	C^+ 90Hz		
	L_1	L_2	L_3
8.5g ∠0°	63.9665	26.1283	78.8703
8.5g ∠15°	62.9611	34.8954	86.1446
8.5g ∠30°	57.2423	42.6974	89.2076
8.5g ∠45°	50.3639	51.5165	90.9024
8.5g ∠60°	43.5482	59.0288	89.8465
8.5g ∠75°	37.6707	65.0294	87.7297
8.5g ∠90°	36.6054	72.4363	87.4850
8.5g ∠105°	27.6120	70.3810	76.3881
8.5g ∠120°	27.9694	74.1862	71.0713
8.5g ∠135°	30.5444	76.0994	63.4475
8.5g ∠150°	35.3333	77.3833	55.1600
8.5g ∠165°	42.0361	75.6699	46.2034
8.5g ∠180°	49.9844	75.0135	38.2035
8.5g ∠195°	55.4830	71.4407	29.1487
8.5g ∠210°	61.3038	67.6013	21.3619
8.5g ∠225°	66.9077	62.4001	18.6300
8.5g ∠240°	71.6353	57.2457	21.5929
8.5g ∠255°	75.8139	50.7012	29.1106
8.5g ∠270°	78.5785	44.5321	38.0906
8.5g ∠285°	79.9388	36.7680	47.2282
8.5g ∠300°	80.5848	30.8797	56.4359
8.5g ∠315°	80.6292	25.9675	65.6722
8.5g ∠330°	79.0303	24.6078	74.1275
8.5g ∠345°	76.2781	26.8263	80.8357
Balanced Rotor	29.0357	26.7303	32.3696

Table 6 Harmonic values of relative phase angle, high frequency h_1.

Case	C^+ 90Hz		
	Θ_{12}	Θ_{13}	Θ_{32}
8.5g ∠0°	174.82	-77.075	-108.10
8.5g ∠15°	-178.5	-80.305	-98.216
8.5g ∠30°	-175.8	-83.950	-91.846
8.5g ∠45°	-176.6	-89.340	-87.251
8.5g ∠60°	178.25	-96.928	-84.826
8.5g ∠75°	172.29	-105.25	-82.461
8.5g ∠90°	159.86	-117.93	-82.216
8.5g ∠105°	148.63	-131.82	-79.552
8.5g ∠120°	128.03	-152.63	-79.342
8.5g ∠135°	111.84	-167.66	-80.500
8.5g ∠150°	98.180	179.09	-80.910
8.5g ∠165°	90.176	174.50	-84.325
8.5g ∠180°	84.296	172.96	-88.641
8.5g ∠195°	81.020	178.35	-97.332
8.5g ∠210°	78.703	-166.82	-114.46
8.5g ∠225°	77.990	-138.40	-143.51
8.5g ∠240°	77.988	-111.39	-170.62
8.5g ∠255°	79.818	-94.088	173.91
8.5g ∠270°	82.625	-85.618	168.24
8.5g ∠285°	88.713	-81.325	170.04
8.5g ∠300°	97.579	-79.224	176.80
8.5g ∠315°	112.82	-78.629	-168.47
8.5g ∠330°	133.72	-78.833	-147.45
8.5g ∠345°	153.65	-80.298	-126.06
Balanced Rotor	-12.90	-7.2849	-5.6192

Table 7 Average influence coefficients

Concept	B^- 30Hz		
	L_1	L_2	L_3
Influence Coefficient (mA/g)	3.3442∠53.6°	3.5159∠294°	3.3813∠174°

Table 8 Comparison of balance masses with applied unbalance, at high frequency h_1 .

Applied unbalance	Balance mass
8.5g ∠180°	8.51g ∠189°
8.5g ∠195°	8.43g ∠197°
8.5g ∠210°	8.94g ∠197°
8.5g ∠225°	9.63g ∠213°
8.5g ∠240°	9.12g ∠223°
8.5g ∠255°	9.82g ∠242°
8.5g ∠270°	9.58g ∠257°
8.5g ∠285°	9.83g ∠286°
8.5g ∠300°	9.82g ∠311°
8.5g ∠315°	9.51g ∠330°
8.5g ∠330°	9.07g ∠344°
8.5g ∠345°	8.91g ∠355°
8.5g ∠0°	8.28g ∠19°
8.5g ∠15°	8.09g ∠29°
8.5g ∠30°	7.71g ∠47°
8.5g ∠45°	7.57g ∠64°
8.5g ∠60°	7.54g ∠75°
8.5g ∠75°	7.71g ∠86°
8.5g ∠90°	7.68g ∠100°
8.5g ∠105°	7.70g ∠113°
8.5g ∠120°	8.00g ∠126°
8.5g ∠135°	8.24g ∠137°
8.5g ∠150°	8.41g ∠148°
8.5g ∠165°	8.53g ∠159°

Table 9 Harmonic amplitudes (mA) at high frequency.

Case	C^+ 90Hz		
	L_1	L_2	L_3
Trial mass 4.3g ∠45°	89.1575	64.4496	117.463
Trial mass 4.3g ∠90°	63.7376	49.7091	96.2145
Trial mass 4.3g ∠135°	41.5683	29.2256	69.4842
Trial mass 4.3g ∠180°	41.3958	12.3781	51.6063
Trial mass 4.3g ∠225°	58.5760	4.6720	54.1722
Trial mass 4.3g ∠270°	82.6952	28.7914	80.0129
Trial mass 4.3g ∠315°	102.255	55.2800	111.258
Applied unbalance 8.5g ∠0°	65.8141	25.6717	79.4410
Balanced Rotor	28.5225	27.2468	33.2415

Table 10 Relative phase angle (°)

Case	C^+ 90Hz		
	Θ_{12}	Θ_{13}	Θ_{32}
Trial mass 4.3g ∠45°	158.46	-93.940	-107.60
Trial mass 4.3g ∠90°	175.80	-88.746	-95.452
Trial mass 4.3g ∠135°	-144.7	-121.33	-122.26
Trial mass 4.3g ∠180°	-79.31	-50.673	-28.640
Trial mass 4.3g ∠225°	106.03	-63.670	-190.30
Trial mass 4.3g ∠270°	138.02	-80.653	-141.32
Trial mass 4.3g ∠315°	145.01	-90.501	-124.49
Applied unbalance 8.5g ∠0°	174.85	-77.623	-107.53
Balanced rotor	-11.44	-5.683	-5.755

Table 11 Balance masses (grams) for each case.

Case	Balance mass
4.3g ∠45°	5.32g ∠178°
4.3g ∠90°	6.97g ∠172°
4.3g ∠135°	8.55g ∠182°
4.3g ∠180°	7.38g ∠182°
4.3g ∠225°	7.78g ∠173°
4.3g ∠270°	8.94g ∠190°
4.3g ∠315°	6.01g ∠208°
Applied unbalance	8.5g ∠180°

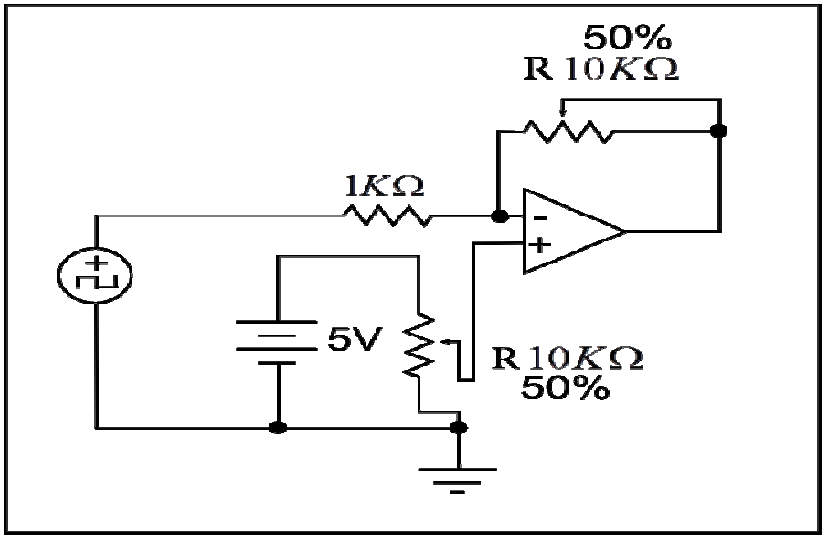

Figure 1 Electric signal conditioner, one channel.

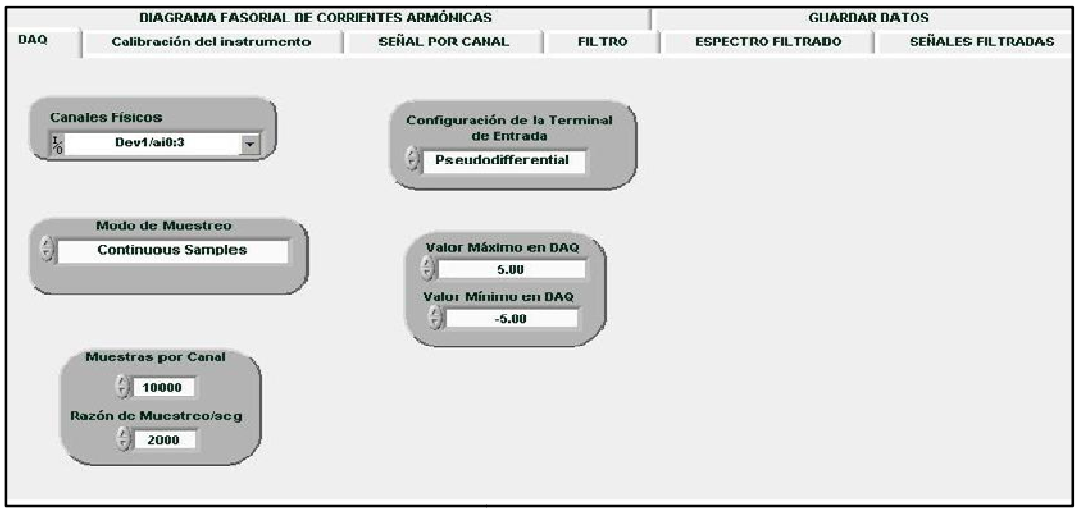

Figure 2 Specifying capture of data

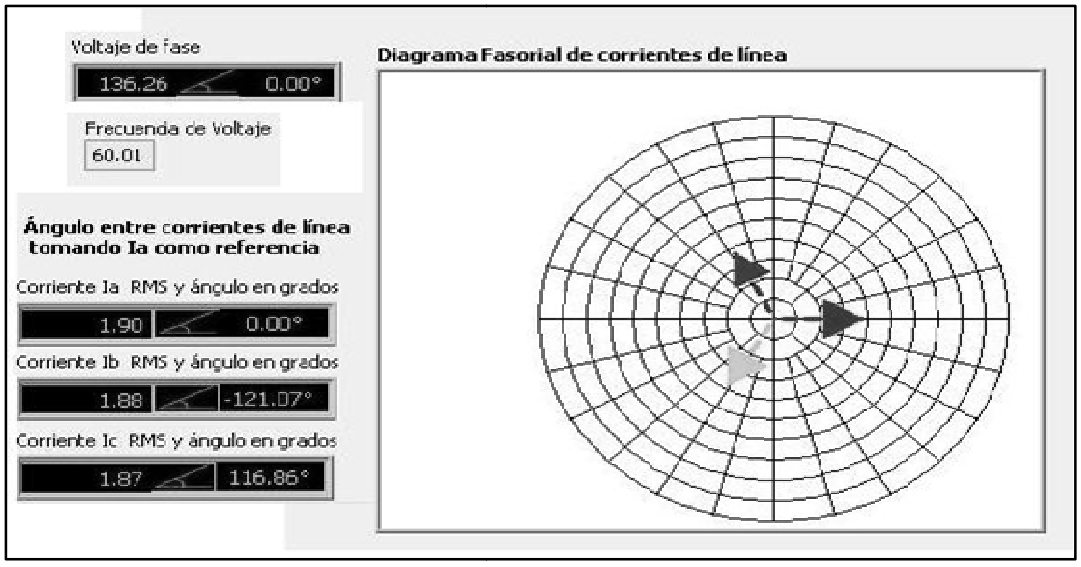

Figure 3 Calibration of instrument

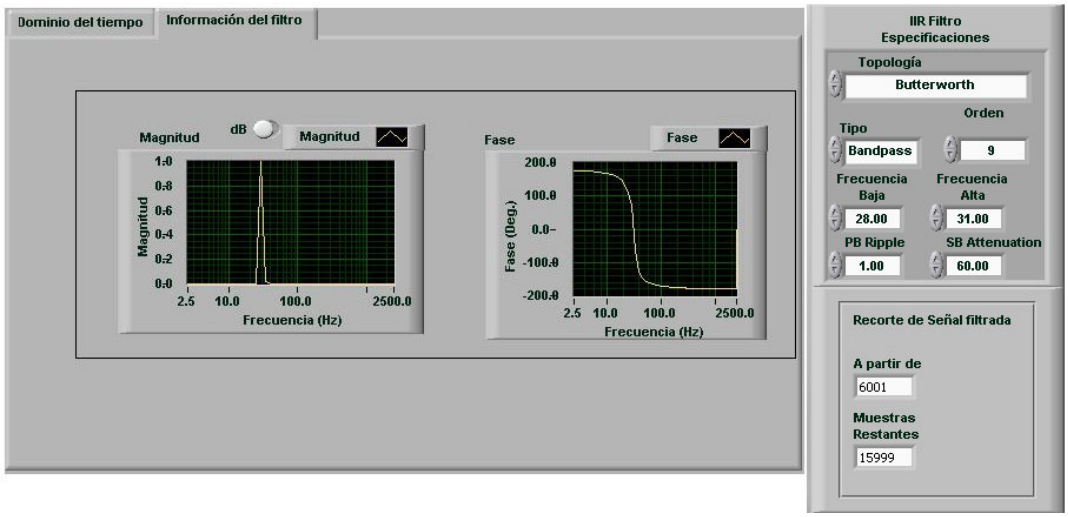

Figure 4 Filter configuration

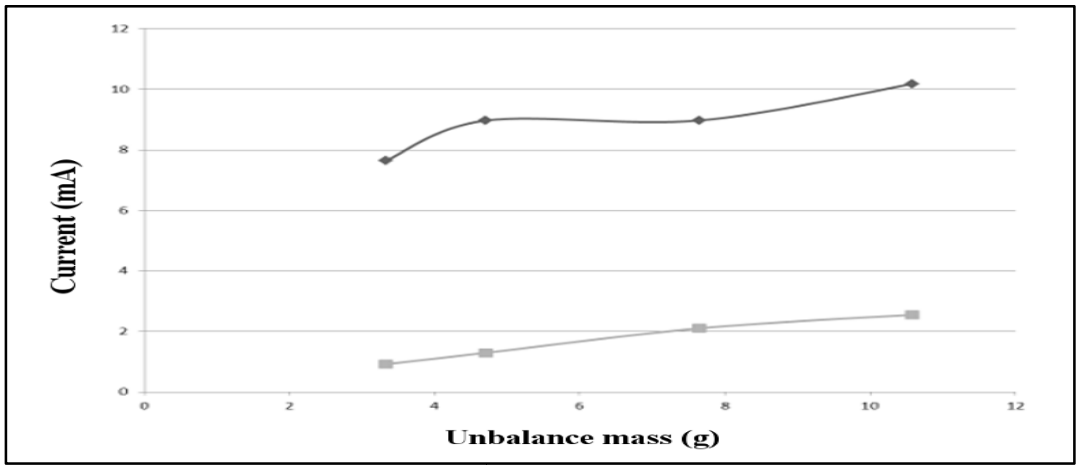

Figure 5Behavior of harmonics with mechanical unbalance in grams.

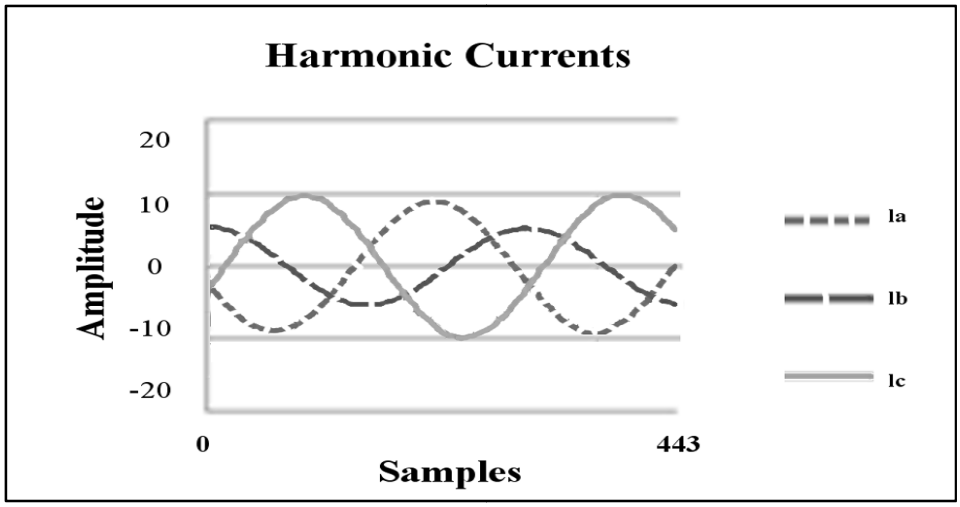

Figure 6 Harmonic time histories for each phase.

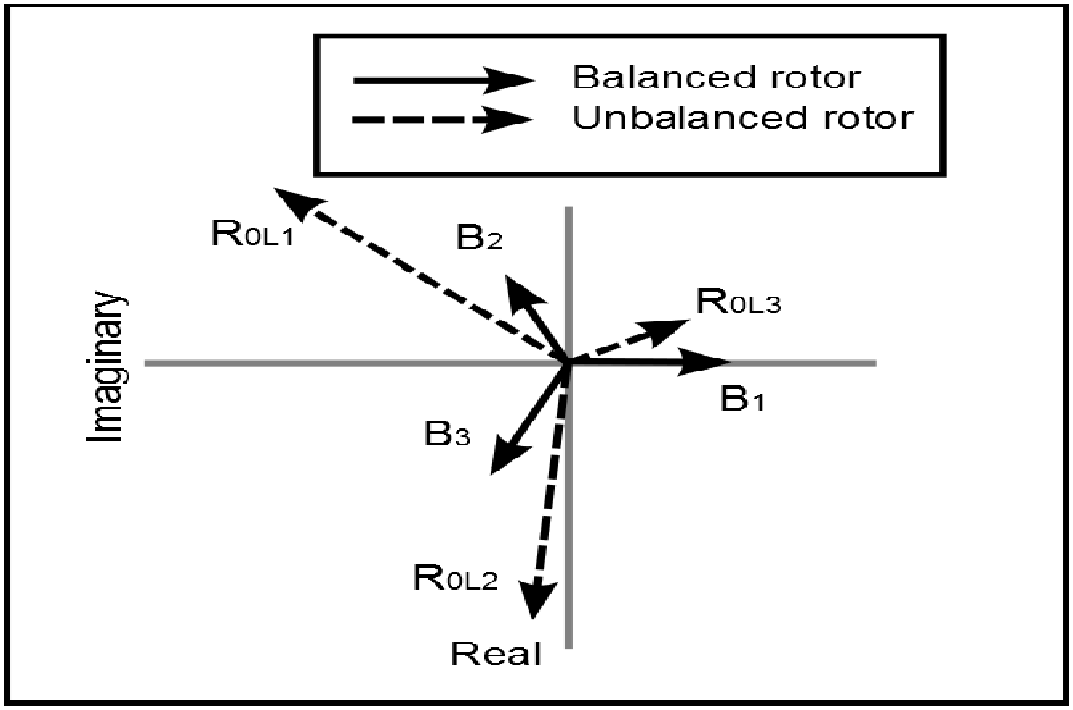

Figure 7 Harmonic vectors.

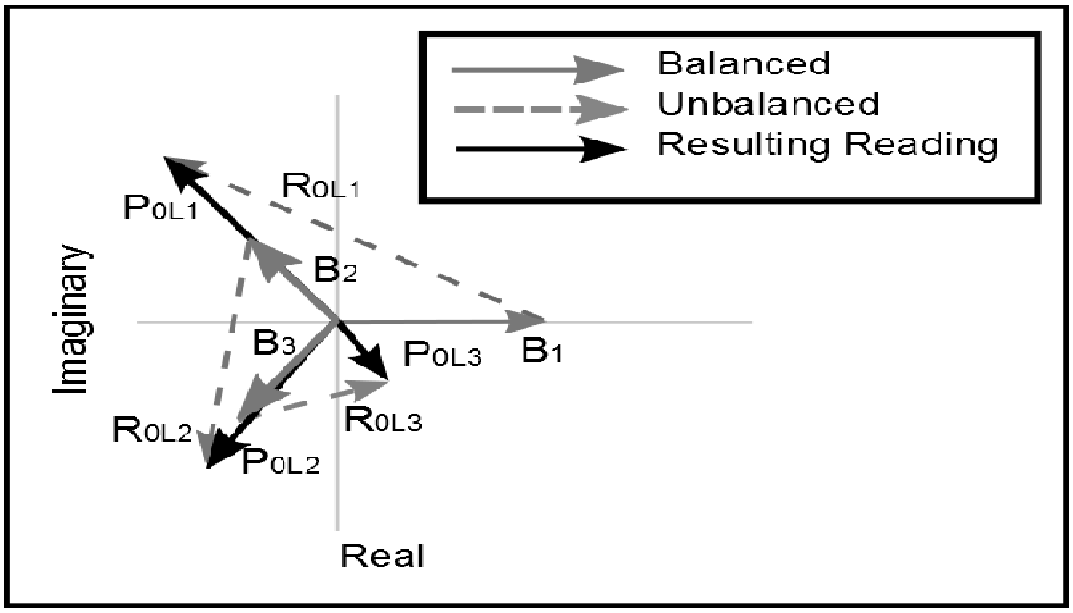

Figure 8 Composition harmonic vectors.

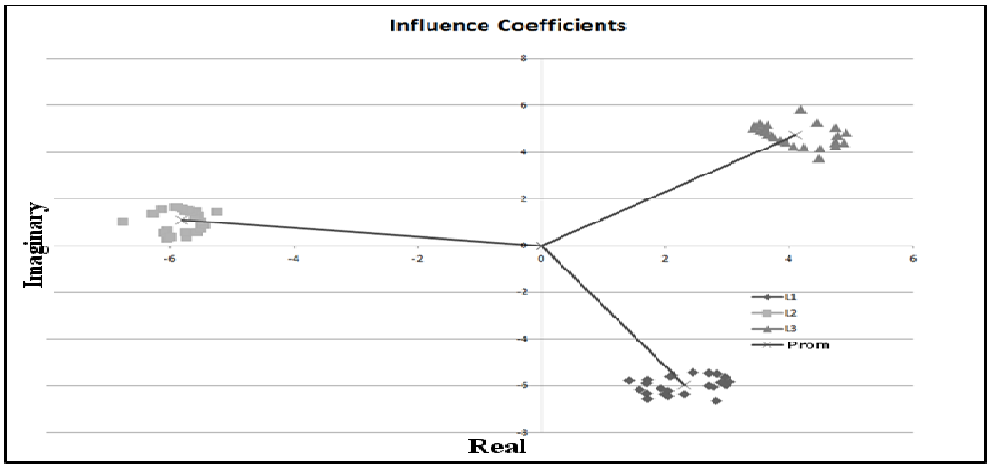

Figure 9 Influence coefficients calculated for each phase.

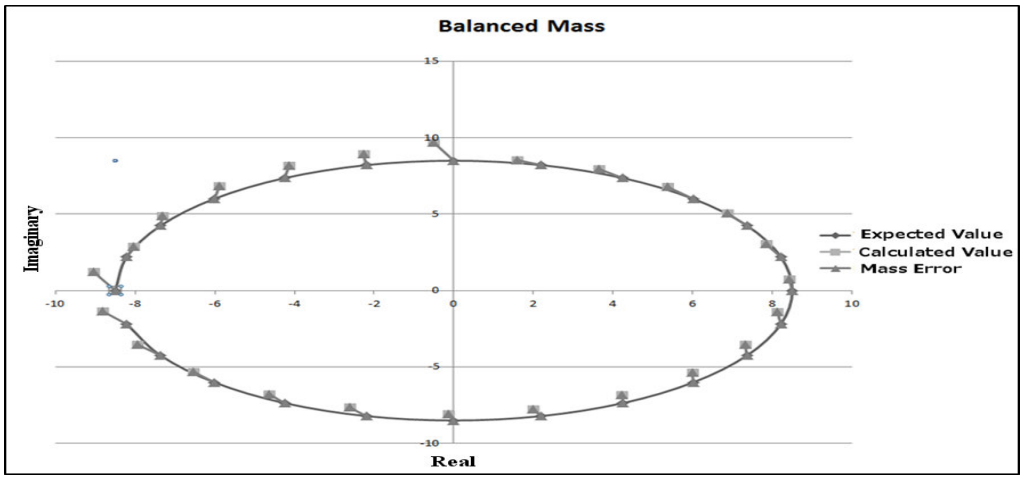

Figure 10 Balanced masses for each applied unbalance